esa ECOSPHERE

Vegetation productivity responds to sub-annual climate conditions across semiarid biomes

Mallory L. Barnes,[1,†] M. Susan Moran,[2] Russell L. Scott,[2]
Thomas E. Kolb,[3] Guillermo E. Ponce-Campos,[2] David J. P. Moore,[1]
Morgan A. Ross,[1] Bhaskar Mitra,[1] and Sabina Dore[3]

[1]*School of Natural Resources and the Environment, University of Arizona, Tucson, Arizona 85719 USA*
[2]*United States Department of Agriculture, Agricultural Research Service, Southwest Watershed Research Center, Tucson, Arizona 85719 USA*
[3]*School of Forestry, Northern Arizona University, Flagstaff, Arizona 86001 USA*

Citation: Barnes, M. L., M. S. Moran, R. L. Scott, T. E. Kolb, G. E. Ponce-Campos, D. J. P. Moore, M. A. Ross, B. Mitra, and S. Dore. 2016. Vegetation productivity responds to sub-annual climate conditions across semiarid biomes. Ecosphere 7(5):e01339. 10.1002/ecs2.1339

Abstract. In the southwest United States, the current prolonged warm drought is similar to the predicted future climate change scenarios for the region. This study aimed to determine patterns in vegetation response to the early 21st century drought across multiple biomes. We hypothesized that different biomes (forests, shrublands, and grasslands) would have different relative sensitivities to both climate drivers (precipitation and temperature) and legacy effects (previous-year's productivity). We tested this hypothesis at eight Ameriflux sites in various Southwest biomes using NASA Moderate-resolution Imaging Spectroradiometer Enhanced Vegetation Index (EVI) from 2001 to 2013. All sites experienced prolonged dry conditions during the study period. The impact of combined precipitation and temperature on Southwest ecosystems at both annual and sub-annual timescales was tested using Standardized Precipitation Evapotranspiration Index (SPEI). All biomes studied had critical sub-annual climate periods during which precipitation and temperature influenced production. In forests, annual peak greenness (EVI_{max}) was best predicted by 9-month SPEI calculated in July (i.e., January–July). In shrublands and grasslands, EVI_{max} was best predicted by SPEI in July through September, with little effect of the previous year's EVI_{max}. Daily gross ecosystem production (GEP) derived from flux tower data yielded further insights into the complex interplay between precipitation and temperature. In forests, GEP was driven by cool-season precipitation and constrained by warm-season maximum temperature. GEP in both shrublands and grasslands was driven by summer precipitation and constrained by high daily summer maximum temperatures. In grasslands, there was a negative relationship between temperature and GEP in July, but no relationship in August and September. Consideration of sub-annual climate conditions and the inclusion of the effect of temperature on the water balance allowed us to generalize the functional responses of vegetation to predicted future climate conditions. We conclude that across biomes, drought conditions during critical sub-annual climate periods could have a strong negative impact on vegetation production in the southwestern United States.

Key words: aboveground net primary production; drought; eddy covariance; Enhanced Vegetation Index (EVI); forests; global change; grasslands; gross ecosystem production; Moderate-resolution Imaging Spectroradiometer; shrublands; U.S. Southwest.

Received 24 April 2015; revised 13 September 2015; accepted 27 October 2015. Corresponding Editor: H. Epstein.

† **E-mail:** mallorybarnes@email.arizona.edu

Introduction

Global climate change is expected to result in altered hydroclimatic conditions which can, in turn, disrupt key ecosystem processes (IPCC 2013), including aboveground net primary production (ANPP) (Zhao and Running 2010). In the southwestern United States (Southwest), warm droughts are projected to increase in frequency and duration (Seager et al. 2007, Cayan et al. 2010, Seager and Vecchi 2010). Already, the early 21st century has brought prolonged drought, warm temperatures, and extreme rainfall events to the Southwest (Easterling et al. 2000, MacDonald 2010). Yet, ecosystem responses to climate variability are not fully understood, and thus the response of ANPP to projected climatic conditions is highly uncertain. Understanding plant functional responses to climate variability is necessary to improve our ability to predict vegetation response to global climate change. Such predictions are essential for assessment of climate change impacts on ecosystem services, land and water resources, and the carbon and water cycles (Backlund et al. 2008).

Regional patterns in vegetation response to climate drivers are ecologically complex and difficult to discern. Distinguishing between natural interannual variability and directional change in vegetation productivity requires a multiyear data record (i.e., 10 yr or more) (Moran et al. 2008). Such long-term studies, often conducted at a single experimental site, can determine the within-site relationship of productivity to climatic variability across time (e.g., Lauenroth and Sala 1992) and discern production legacies during drought (Peters et al. 2012).

Interannual variation in vegetation productivity within-sites is thought to be broadly explained by both life history and biogeochemical interactions (Huxman et al. 2004). However, a global analysis of the impact of drought on satellite, dendrochronological and in situ estimates of vegetation productivity indicates that empirical drought response mechanisms underlying these dynamics vary between ecosystem types (Vicente-Serrano et al. 2013). Warm drought conditions caused widespread mortality in U.S. Southwest forests (Breshears et al. 2005, Allen et al. 2010), but caused shifts in the functional response of ANPP to precipitation in Southwest desert grasslands (Moran et al. 2014). The most important inter-annual climatic drivers between different ecosystem types are not resolved. Some cross-biome studies conclude that inter-annual variability in vegetation productivity is insensitive to variation in precipitation (Knapp and Smith 2001, Hsu et al. 2012), whereas others report strong relationships between productivity and precipitation variation across biomes (Fang et al. 2001, Ma et al. 2013).

The interpretation of inter-annual effects of drought may be further complicated by within-year or intra-annual variation in precipitation and temperature. In grasslands, the timing of interannual variation in climate drivers affects ecological processes (Craine et al. 2009, 2012, Craine 2013). Grassland productivity showed differential sensitivity to precipitation and temperature at distinct time periods during the growing season (Craine et al. 2012, Craine 2013). Such studies underscore the need to consider not only the magnitude, but also the sub-annual timing of precipitation and temperature. Although the existence of these "critical climate periods" have been identified in grasslands, further exploration of the effects of sub-annual climate conditions in shrubland and forest biomes is necessary.

Many studies have considered the functional relationships between climatic drivers and productivity (e.g., Vicente-Serrano et al. 2013, Zhang et al. 2015). To investigate plant functional responses across a range of ecosystem types in the Southwest, we attempt to identify mechanisms driving variability in these responses. We focused here on those mechanisms that underlie vegetation response to climate variability, recognizing that plant physiology and biogeochemical interactions further underlie these relationships. Using a combination of decade-long observations to address interannual variability and fine-temporal-resolution in situ data to identify mechanisms across multiple ecosystem types, it is possible to generalize vegetation response to climate variability. For example, Ma et al. (2013) coupled ground measurements of photosynthesis with 13 yr of satellite observations of vegetation greenness to characterize spatial and temporal variability in savanna phenology across an ecological rainfall gradient in Australia. Here, we investigate inter- and intra-annual changes in gross ecosystem productivity and ecosystem phenology as ecological mechanisms contributing to

previously observed patterns in responses of aboveground net productivity (Ponce-Campos et al. 2013, Moran et al. 2014) and explore their environmental controls empirically.

This study assessed long-term dynamics in productivity at multiple sites across biomes, and then interpreted those dynamics based on mechanisms identified with high-temporal-resolution in situ measurements at each site. We used satellite observations of the Enhanced Vegetation Index (EVI) from the Moderate-resolution Imaging Spectroradiometer (MODIS) to estimate peak greenness (EVI_{max}) at eight eddy covariance flux tower sites from the Ameriflux network. Sites were chosen across the Southwest and represented several dominant biomes in arid and semiarid ecosystems: grasslands, shrublands, and forests. First, we developed biome-specific models of interannual EVI_{max} in relation to annual and sub-annual climatic drivers including precipitation and temperature based on long-term (13-yr; 2001–2013) EVI measurements at each site. We derived four empirical models from recent influential studies of the relationship between vegetation production and climate drivers. We then determined the most parsimonious model that explained variation in EVI_{max} for each biome. Then, we interpreted these results using daily estimates of gross ecosystem production (GEP) measured with the eddy covariance method. This coupled approach afforded us the unique ability to generalize responses of plant productivity to changing hydroclimatic conditions across Southwest ecosystem types. The study was framed in the context of the 21st century drought, a prolonged drought coupled with warm temperatures that is thought to be similar to predicted future conditions in the Southwest (MacDonald 2010).

Materials, Methods, and Models

Study sites

This study focused on eight experimental sites from the Ameriflux national eddy covariance network (http://ameriflux.lbl.gov/). These study sites represent a variety of Southwest biomes, elevations, and varied precipitation and temperature regimes (Table 1). Locations include three forest sites in New Mexico and Arizona, three shrubland sites in New Mexico and Arizona, and two grassland sites in New Mexico and Arizona (Fig. 1). The sites range in elevation from 1116 m at US-Srm to 3003 m at US-Vcm, in mean annual precipitation (MAP) from 242 mm at US-Seg to 659 mm at US-Fuf, and in mean annual temperature (MAT) from 5.4°C at US-Vcm to 18.4°C at US-Srm. Study sites include two sets of paired grassland-shrubland sites: US-Seg and US-Ses at the Sevilleta National Wildlife Refuge and LTER site, and US-Wkg

Table 1. Characteristics, data availability, and locations of the eight Ameriflux sites used in this study.

Biome	Site	IGBP classification	Fluxnet ID	Elevation (m)	MAT (°C)	MAP (mm)	Lat (°)	Long (°)	Flux data range
Forest	Flagstaff Unmanaged Forest	Evergreen needleleaf forest	US-Fuf	2180	7.8	659	35.09	−111.76	2006–2010
	Valles Caldera Mixed Conifer	Evergreen needleleaf forest	US-Vcm	3003	5.4	605	35.89	−106.53	Not used
	Valles Caldera Ponderosa Pine	Evergreen needleleaf forest	US-Vcp	2542	5.8	585	35.86	−106.6	Not used
Shrubland	Santa Rita Mesquite Savanna	Woody savanna	US-Srm	1116	18.4	425	31.82	−110.87	2004–2013
	Lucky Hills Shrubland	Open shrubland	US-Whs	1372	16.8	360	31.74	−110.05	2007–2013
	Sevilleta Desert Shrubland	Open shrubland	US-Ses	1593	13.6	243	34.34	−106.74	Not used
Grassland	Kendall Grassland	Grassland	US-Wkg	1531	16	404	31.74	−109.94	2004–2013
	Sevilleta Desert Grassland	Grassland	US-Seg	1622	13.6	242	34.36	−106.7	Not used

Notes: International Geosphere-Biosphere Programme (IGBP) vegetation classification for each site is presented. All site data were compiled from publicly available information provided by Ameriflux principal investigators to the Ameriflux Site and Data Exploration System provided and maintained by Oak Ridge National Laboratory (ORNL) (http://ameriflux.ornl.gov/), except for mean annual temperature (MAT) and mean annual precipitation (MAP). MAT and MAP were derived from Daymet long-term daily climate data (1980–2013) extracted from the 1 × 1 km pixel closest to the flux tower. Daymet data were obtained through the ORNL Distributed Active Archive Center (DAAC).

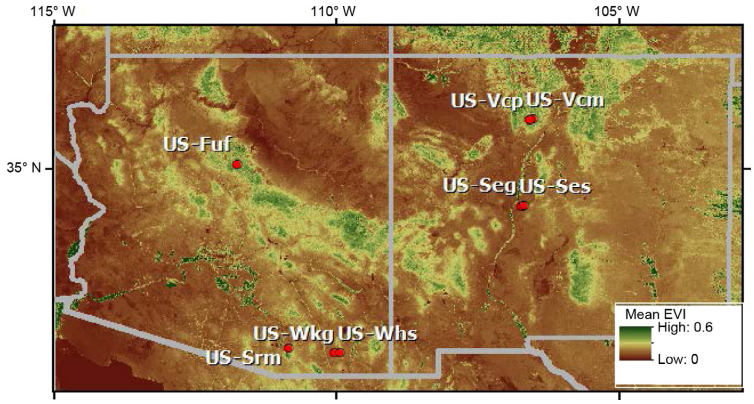

Fig. 1. Locations of the eight Ameriflux sites across the Southwest United States, overlain on an image of the mean Enhanced Vegetation Index (EVI, 2.25 × 2.25 km) over all years in the study period (2001–2013). US-Seg and US-Ses are Sevilleta Desert Shrubland and Desert Grassland, respectively. US-Fuf is Flagstaff Unmanaged Forest, US-Srm is Santa Rita Mesquite Savannah, US-Wkg is Kendall Grassland, US-Whs is Lucky Hills Shrubland. US-Vcp and US-Vcm are Valles Caldera Ponderosa Pine Forest and Mixed Conifer Forest, respectively, and US-Seg and US-Ses are Sevilleta Desert Shrubland and Desert Grassland, respectively.

and US-Whs at the Walnut Gulch Experimental Watershed. The US-Vcm and US-Vcp are paired mixed-conifer/ponderosa woodland sites.

Climate data

Daily precipitation and temperature data for each site were obtained from the Daymet data set through the Oak Ridge National Laboratory Data Archive and Distribution Center (ORNL DAAC) (http://daymet.ornl.gov/). The Daymet data set provides estimates of daily meteorological parameters over North America on a 1 × 1 km grid (Thornton et al. 1997). Estimates are derived from meteorological station data and interpolated and extrapolated to provide continuous estimates of precipitation and temperature data across the conterminous United States (Thornton et al. 1997). Data are available for the last 34 yr, from 1980 through 2013. Daily precipitation, minimum temperature, and maximum temperature data were extracted for the 1 × 1 km pixel encompassing each Ameriflux site. Total annual precipitation (P_T) was computed as a sum of daily precipitation in the hydrologic year (01 October to 30 September).

SPEI

The Standardized Precipitation-Evapotranspiration Index (SPEI) uses potential evapotranspiration (PET) and precipitation to characterize the drought conditions in a given area across dynamic timescales. Because it accounts for the effect of increased temperatures on the water balance, the SPEI is considered to be a better predictor of changes in ecological response to drought than other drought indices, especially in the summer (Vicente-Serrano et al. 2012). Additionally, the SPEI is multiscalar, allowing calculations at a range of timescales ranging from 1 to 48 months to examine impacts of both short-term and long-term water deficits (Vicente-Serrano et al. 2010). The SPEI requires a calibration period to determine the average water balance (precipitation minus PET) and then calculates deviations from the average water balance. Negative SPEI values represent drought conditions and positive SPEI values represent wet conditions.

The SPEI was included as a predictor at 1- to 12-month timescales in this analysis. The SPEI was computed at the end of the growing season using three endpoints (September, August, and July). In all, 36 SPEI models (12 timescales × 3 endpoints) were calculated for each biome.

The SPEI was computed from the Daymet data at 1 × 1 km resolution using a software package housed in the R language (R version 3.0.2) and environment for statistical computing (R Core Team 2013). Daily Daymet data were aggregated to monthly for the computation of PET and SPEI. The tools for calculating PET and SPEI are

available in the package "SPEI" (Beguería and Vicente-Serrano 2013). We used the function "thornthwaite" to calculate PET according to the Thornthwaite equation (Thornthwaite 1948), and the function "spei" to calculate SPEI from PET and daily precipitation. Daytime average temperature was estimated from daily T_{max} and T_{min} from the equation for daylight weighted average air temperature (Running et al. 1987). The calibration period for SPEI was January 1980 to December 2013.

To put the 21st century drought in historic context, SPEI was also obtained from the SPEI Global Drought Monitor (http://sac.csic.es/spei/map/maps.html) at 0.5 degrees from January 1950 to December 2010. At this coarse resolution, the paired US-Seg and US-Ses sites and the US-Vcm and US-Vcp sites fell within the same SPEI tile. The calibration period for SPEI from the Global Drought Monitor was January 1950 to December 2010. Calculation of PET was based on the Thornthwaite equation (Thornthwaite 1948).

For the purposes of explanation, SPEI > 0.5 was considered a wet spell, 0.5 > SPEI ≥ −0.5 is normal, and SPEI < −0.5 was moderate drought, and SPEI < −1.3 was severe drought. These drought classifications were based on the Drought Severity Classification for the Standardized Precipitation Index (SPI) used by on the U.S. Drought Monitor (http://droughtmonitor.unl.edu/AboutUs/ClassificationScheme.aspx).

Remotely sensed EVI

We used satellite observations of the EVI from the MODIS to determine peak greenness. A widely used measure of greenness, EVI is defined as

$$\mathrm{EVI} = G\frac{\rho_{\mathrm{NIR}} - \rho_{\mathrm{red}}}{\rho_{\mathrm{NIR}} + C_1\rho_{\mathrm{red}} - C_2\rho_{\mathrm{blue}} + L} \quad (1)$$

where ρ_{NIR}, ρ_{red}, and ρ_{blue} are atmospherically corrected surface reflectances for the near-infrared, red, and blue bands, L is the canopy background adjustment, C_1 and C_2 are the coefficients of the aerosol resistance term, and G is a gain factor (Huete et al. 2002).

MODIS EVI data (MOD13Q1) were averaged over an area of 9 × 9 MODIS pixels (2.25 × 2.25 km) surrounding the eddy covariance flux tower at each site for the full MODIS time series (2001–2013). There were 23 EVI scenes per year and 13 yr, totaling 299 EVI scenes for each site. Data were smoothed using TimeSat software (Jönsson and Eklundh 2004).

Although previous studies have used integrated annual EVI (iEVI) as a surrogate for annual ANPP (e.g., Ponce-Campos et al. 2013, Zhang et al. 2013, Moran et al. 2014), recent research suggests that evergreen forests have low spectral sensitivity to water stress (Sims et al. 2014). However, satellite observations of forest greenness during the peak of the growing season were correlated with forest drought stress (Williams et al. 2013). Here, we use the mean of the four consecutive maximum EVI observations in the growing season (EVI_{max}) as an estimate of peak greenness (Fig. 2).

Flux data

Ameriflux sites use eddy covariance techniques to continuously measure CO_2 exchange between ecosystems and the atmosphere aggregated to 30–60 min intervals. Additionally, climate variables are measured at each flux tower, including precipitation, temperature, and vapor pressure deficit (VPD). Daily gap-filled GEP estimates and climate variables were obtained directly from site administrators. We used data from 4 flux sites with long-term (≥5 yr) data records: US-Fuf, US-Srm, US-Wkg, and US-Lhs (Table 1). There were 5 yr of GEP data available from US-Fuf, 10 yr from US-Srm, 7 yr from US-Whs, and 10 yr from US-Wkg.

Gross ecosystem production was derived from the following equation:

$$\mathrm{GEP} = \mathrm{R_{eco}} + \mathrm{NEE} \quad (2)$$

where NEE is net ecosystem exchange of CO_2, R_{eco} is ecosystem respiration, and GEP is gross ecosystem production. NEE is calculated directly from measured carbon dioxide flux and then partitioned into GEP and R_{eco} (for site-specific methods see Dore et al. 2008, Scott et al. 2010). Daily GEP estimates were used for interpretation, and specifically, to discern mechanisms underpinning modeling results.

Relationships among vegetation productivity, GEP and EVI_{max}

Although both GEP and EVI_{max} reflect carbon uptake by plants, EVI is a greenness index and GEP measures total photosynthetic uptake per unit of time. Plants make frequent

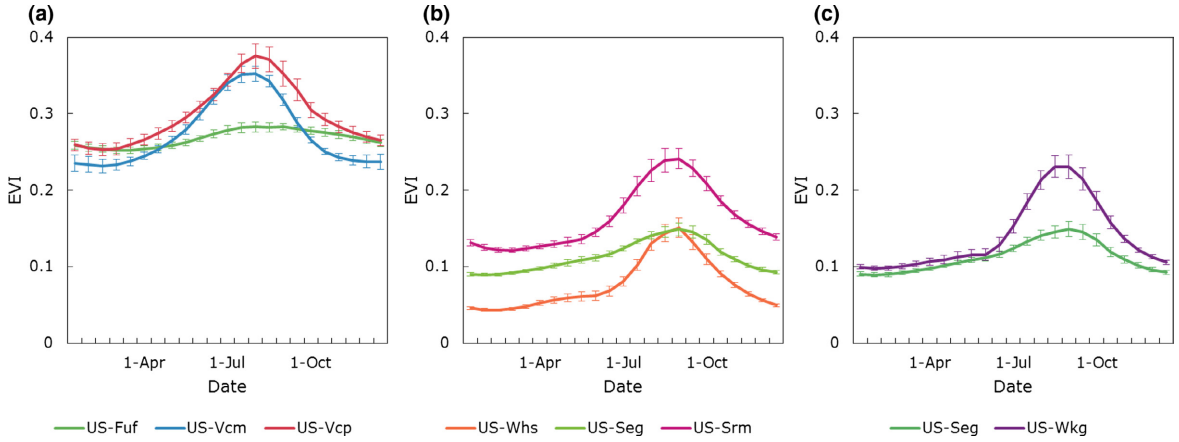

Fig. 2. Sixteen-day ensemble averages of Moderate-resolution Imaging Spectroradiometer (MODIS) Enhanced Vegetation Index (EVI, 2.25 × 2.25 km) for all sites used in this study grouped by biome: (a) forests (b) shrublands and (c) grasslands. Data are averages (±1 standard error) across all years used in the study (2001–2013). Ensemble averages for US-Vcm and US-Vcp are for 2001–2012 only due to the 2013 Thompson Ridge Fire in the Valles Caldera National Preserve.

diurnal adjustments in response to daily or sub-daily fluctuations in environmental conditions, such as opening and closing their stomata in response to VPD. Satellite EVI does not measure these fundamental plant mechanisms, but is instead sensitive to slowly changing, dramatic variations in greenness. Further, the 16-d temporal resolution of EVI is too coarse to incorporate daily or sub-daily plant mechanisms. Because the flux measurements are in situ and at fine temporal scale, these diurnal adjustments are accounted for in the measured GEP. Consequently, we recognize in this study that GEP and EVI_{max} are different yet complementary measures of vegetation productivity.

MODIS EVI is a 16-d composited product. To maximize temporal synchronization between daily GEP and 16-d EVI, we added 16 d to the end of the EVI_{max} range for each year. Daily GEP values in the time period of EVI_{max} + 16 d were then summed to calculate GEP_{max}.

The time series of EVI at the US-Fuf site showed little seasonal variation in greenness (Fig. 2a) and was thus not included in the annual models, but US-Fuf was still used for analyses involving GEP. The 2013 Thompson Ridge Fire in the Valles Caldera National Preserve affected both the US-Vcp and US-Vcm sites, thus 2013 was not included in the annual models for either site.

Modeling

To determine the relative importance of climate drivers and legacies in different ecosystem types, four models were evaluated. To allow for meaningful comparisons across sites, climatic variables and EVI values were standardized in these models, where the standardized values were the deviation of the *i*-year value from the 13-yr average in units of standard deviation (σ). For a given variable X,

$$X_S = \frac{X_i - \overline{X}}{\sigma_X} \quad (3)$$

Because SPEI is already standardized to the mean of the calibration period for a given site, SPEI was not standardized by Eq. 3.

The first model was based on recent evidence suggesting that plant communities across diverse biomes share an intrinsic sensitivity to water availability (Ponce-Campos et al. 2013). In dry years, ecosystem water-use efficiency (WUE_E; above-ground net primary production/evapotranspiration) converged to a common maximum cross-biome WUE_E (Ponce-Campos et al. 2013). During drought, ecosystems that are normally constrained by resources other than water (e.g., light, nutrients) can become water-limited (Jenerette et al. 2012). Thus, we inferred that during the persistent 21st century

drought in the Southwest, plant communities across biomes would behave as if they were water-limited. Using EVI_{max} as a measure of vegetation productivity, we expect that across biomes, $EVI_{max} = f(P_T)$. Thus, using standardized values for cross-site comparison, we proposed that

$$EVI_{max_{S(y)}} = b_0 + b_1 P_{T_{S(y)}} \quad (4)$$

where b_0 and b_1 are empirically derived coefficients specific to this equation, P_{TS} is standardized total annual precipitation, and the subscript y represents the current year.

Sala et al. (2012) suggested that in grasslands, legacies of wet and dry years influenced annual vegetation productivity. They proposed that current-year ANPP was based on both current-year P_T and ANPP in the previous year. Experimental manipulations provided support for legacy effects in grasslands (Reichmann et al. 2013), and in a Chihuahuan Desert shrubland, legacy effects in underlying grasses were found after several consecutive wet years (Peters et al. 2014). Using EVI_{max} as a measure of vegetation productivity, we expect that in grasslands, $EVI_{max_{(y)}} = f(P_{T(y)}, EVI_{max_{(y-1)}})$, where $EVI_{max_{(y-1)}}$ is the previous-year's EVI_{max}. This led to the second model for this study, where

$$EVI_{max_{S(y)}} = b_0 + b_1 P_{T_{S(y)}} + b_2 EVI_{max_{S(y-1)}} \quad (5)$$

where b_0, b_1, and b_2 are empirically derived coefficients specific to this equation, P_{TS} is standardized total annual precipitation, and the subscript y represents the current year.

Southwest forest growth depends on snowmelt from winter precipitation (Kerhoulas et al. 2013), which replenishes soil water in the spring. In the spring and summer, high evaporative demand associated with warm temperatures causes stomatal closure in trees, which if prolonged, can lead to carbon starvation and mortality (Adams et al. 2009). Williams et al. (2013) determined an index of forest drought stress (FDSI) that was based on warm-season VPD and cool-season (November through March) precipitation. Warm-season VPD was defined as the average of VPD from August–October of the previous year and May–July of the current year. An equivalent relation specific to this study was derived by using EVI_{max} as a proxy for forest production and maximum temperature (T_{max}) in place of VPD. VPD is largely determined by temperature in the Southwest (Weiss et al. 2009), and T_{max} was found to predict nearly the same variation in the FDSI as VPD (Williams et al. 2013). Adapting this equation, we expected that in forests, $EVI_{max} = f(P_{cool}, T_{max_{warm}})$, where P_{cool} is the average of precipitation from November through December of the previous year and January through March of the current year, and $T_{max_{warm}}$ is the mean daily maximum temperature from August–October of the previous year and May–July of the current year. The third model used in this study was

$$EVI_{max_{S(y)}} = b_0 + b_1 P_{cool\,S} + b_2 T_{max_{warm\,S}} \quad (6)$$

where b_0, b_1, and b_2 are empirically derived coefficients specific to this equation.

The effect of temperature on production in the Southwest is not fully understood. Increased temperatures combined with reduced precipitation exacerbate the effects of drought in the Southwest (Breshears et al. 2013), and if prolonged, can cause mortality events and alter ecosystem function (Breshears et al. 2005). Plants do not experience precipitation and temperature separately, so it is reasonable to expect that the combined effect of these climate drivers will affect vegetation production. Additionally, seasonal temperature and precipitation are likely to influence vegetation production in addition to annual precipitation. For example, Southwest forests are dependent on winter precipitation, but many Southwest grasslands and shrublands are dependent on the heavy rains brought by the North American Monsoon in late summer. We expect that SPEI will predict interannual variation in EVI_{max} for two reasons: first, because it accounts for the combined effect of temperature and precipitation on production, and second, because it allows us to pinpoint the dominant timescale that influences vegetation production for each biome. We expect that across biomes, $EVI_{max} = f(SPEI n_m)$, where SPEI is calculated in month m at a n-month timescale and n is the dominant timescale (in months) that influences vegetation production. The dominant timescale (n) was determined as the SPEI timescale that

was most highly correlated with $EVIs_{max_{(y)}}$ for each biome. The fourth model is a simple linear relation, where

$$EVI_{max_{S(y)}} = b_0 + b_1 SPEIn_m \quad (7)$$

where b_0 and b_1 are empirically derived coefficients specific to this equation.

Statistics

Sites were grouped by biome as described in Table 1. We fit all models (Eqs. 4–7) for the two combined forest sites, three combined shrubland sites, and two combined grassland sites. The best model was selected based on Akaike's Information Criterion adjusted for small sample sizes (AIC_c) and the coefficient of determination (r^2) (Burnham and Anderson 2002). An additional parameter was only included in the model if its addition reduced the AIC_c by 2 or more (Burnham and Anderson 2002). The SPEI, because it is calculated from PET and precipitation, was considered to have two parameters for AIC analysis. If two models had the same number of parameters, the model with the lowest AIC_c was selected.

Statistical analyses were performed in R version 3.0.2 (R Core Team 2013). Regression analyses were performed using the base linear modeling functions (R Core Team 2013), and break point analyses were performed using the "segmented" package (Mueggo 2008). AIC_c values were calculated using the "$AIC_{cmodavg}$" package in R (Mazerolle 2013).

Results

Early 21st century drought

To determine if the study sites experienced altered hydroclimatic conditions associated with the 21st century drought, we compared historic SPEI (1950–1999) to early 21st century SPEI values (2000–2013). Based on the annual SPEI values provided by the Global Drought Monitor, all sites experienced drought during the study period (2001–2013) (Fig. 3). All sites experienced at least 2 yr of extreme drought, and US-Srm had extreme or moderate drought for 10 yr of the 13-yr study period. Annual SPEI during the early 21st century (2000–2013) was significantly lower than SPEI from 1950 to 1999 ($P < 0.05$) at all sites except for US-Seg and US-Ses in New Mexico, where there was no significant difference between the two time periods (Table 2). Here, SPEI calculated from the Global Drought Monitor was used to provide historic context to our study. In all subsequent mentions of SPEI, values were calculated from 1-km Daymet data.

Using SPEI calculated from Daymet data at 1-km resolution from 1980 to 2013, we confirmed that all study sites experienced prolonged drought and increased temperatures associated with altered hydroclimatic conditions in the early 21st century (Table 3). All sites experienced prolonged dry conditions (SPEI < 0) in the early 21st century ranging from 5 to 8 yr, whereas dry conditions in the late 20th century lasted only 1–3 yr. The difference between average temperature from 1980 to 1999 and from 2000 to 2013 (ΔT) was positive (i.e., increased temperatures during the early 21st century) in both the warm season (April–September) and the cool season (October–March). The magnitude of ΔT was larger in the warm season than in the cool season; warm-season temperature during the 21st century increased by 1.25°, 0.74°, and 0.66°C in forests, shrublands, and grasslands, respectively (Table 3).

Dynamic timescale of SPEI

Rather than report model results for all SPEI timescales calculated at July, August, and September (48 models), we report only the dominant SPEI timescale for each biome defined by the highest correlation with $EVIs_{max}$. The dynamic timescale of SPEI, however, provides important information about the dominant timescales at which drought has the strongest influence on vegetation production (Fig. 4). In forests, the correlation between SPEI and $EVIs_{max}$ was highest for $SPEI9_{Sep}$, the 9-month SPEI calculated in September (i.e., January–September) (Fig. 4a). The correlation for shrubland was highest for $SPEI2_{Aug}$, the 2-month SPEI calculated in August (i.e., July–August) (Fig. 4b), and for grassland, the correlation was highest for $SPEI3_{Sep,}$ the 3-month SPEI calculated in September (July–September) (Fig. 4c).

The definition of timescales at which drought has the strongest influence on vegetation

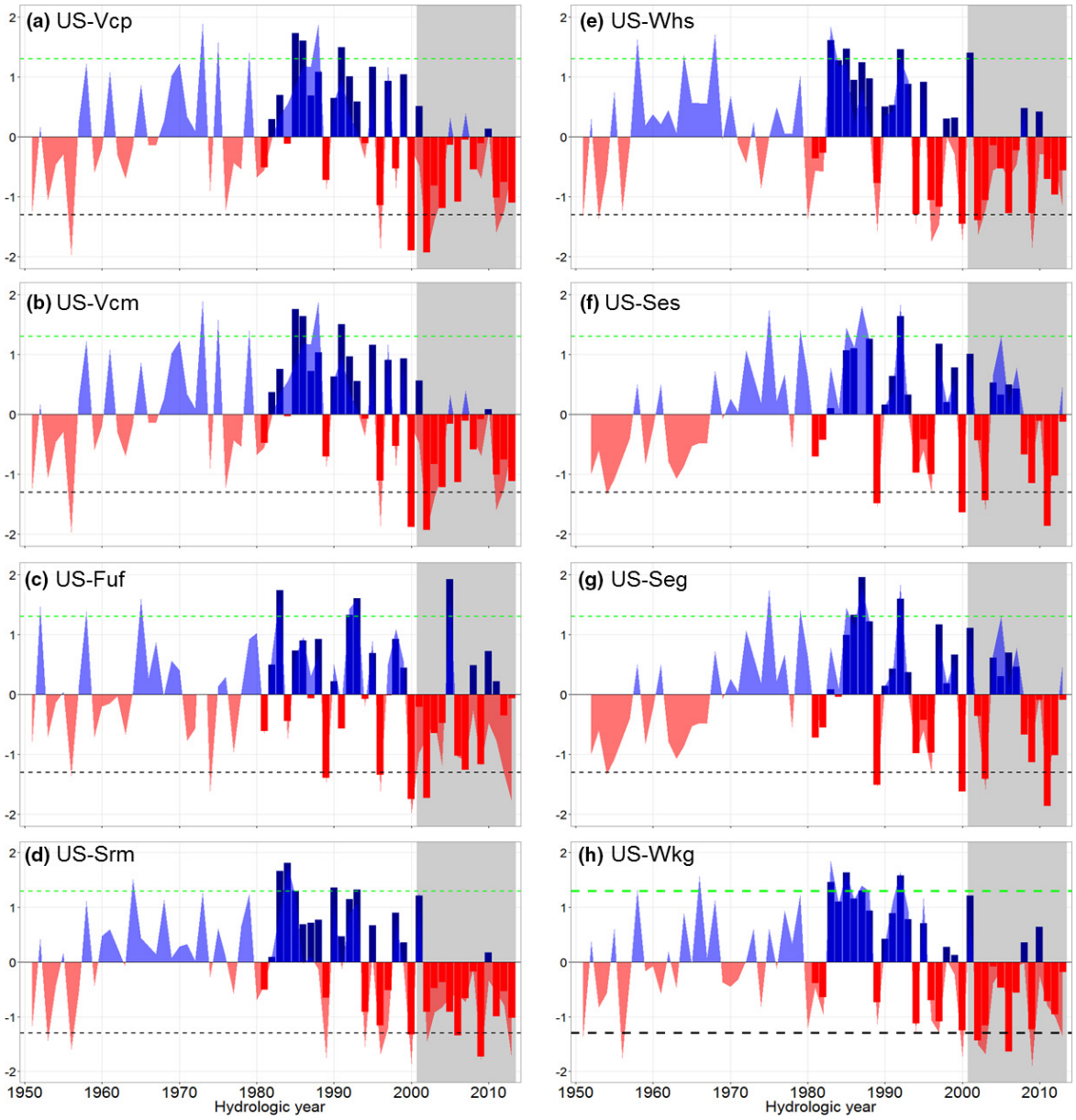

Fig. 3. Annual SPEI from 1950 to 2013 for all sites. Lines shaded with red above and blue underneath are 0.5° SPEI from 1950 to 2013 obtained from the SPEI Global Drought Monitor. Bars are SPEI from 1980 to 2013 calculated from 1 km Daymet data for each site. Twelve-month SPEI was computed at the end of the hydrologic year in September. Red indicates that SPEI is less than zero (dry) and blue indicates that SPEI is greater than zero (wet). Dashed lines represent wet spells (SPEI > 1.3) and extreme drought conditions (SPEI < −1.3). The gray shaded region of the graph indicates the time period examined in this study (2001–2013).

production inspired a revisit of the drought conditions at our sites during the early 21st century (Table 4). The number of drought years (SPEI < −0.5) at the dominant timescale for each site was compared to the number of drought years at the annual timescale. The SPEI in the early 21st century (2000–2013) at the dominant timescale for forest sites ($SPEI9_{Sep}$) indi-

cated that there were more drought years than defined by annual SPEI at all three forest sites. When the dominant timescale was considered, US-Fuf, US-Vcm, and US-Vcp had 1, 2, and 2 more years of drought, respectively. In shrublands, consideration of the dominant timescale ($SPEI2_{Aug}$) indicated fewer years of drought than did annual SPEI (Table 4). There were 3, 2, and 2 fewer drought years as defined by the dominant timescale for US-Srm, US-Ses, and US-Whs, respectively. In grasslands, the number of drought years indicated by SPEI at the dominant timescale ($SPEI3_{Sep}$) was similar to the number of drought years indicated by annual SPEI (Table 4). Considering the dominant timescale indicated one less drought year for both US-Wkg and US-Seg compared to annual SPEI (Table 4). Overall, considering the annual SPEI rather than SPEI at the dominant timescale underestimates the number of drought years in forests and overestimates the number of drought years in shrublands. These sub-annual calculations of SPEI are more indicative of the climate conditions that influence vegetation production in Southwest ecosystems than annual SPEI.

Table 2. Differences between the historic mean SPEI (1950–1999) and mean SPEI during the early 21st century (2000–2013) using SPEI calculated from the Global Drought Monitor for the eight study sites.

Site	Historic mean SPEI (1950–1999)	21st century mean SPEI (2000–2013)
US-Wkg	0.154	−0.774*
US-Whs	0.148	−0.676*
US-Srm	0.164	−0.796*
US-Seg & US-Ses	0.012	−0.148
US-Fuf	0.185	−0.920*
US-Vcm & US-Vcp	0.157	−0.790*

Note: Asterisks represent significant differences ($p < 0.05$) between 21st century and historic mean SPEI values.

Modeling results

The SPEI calculated in month m at an n-month timescale is described here as $SPEIn_m$, where SPEI calculated in September at a 9-month timescale is referred to as $SPEI9_{Sep}$. Similarly, standardized precipitation and maximum temperature over the dominant timescale are described as Pn_{mS} and $T_{max_{mS}}$ where, for example, standardized precipitation averaged over at a 9-month timescale from January to September is referred to as $P9_{SepS.}$

For Southwest forests, the model based on SPEI calculated in September at a 9-month timescale ($SPEI9_{Sep}$) was selected ($AIC_c = 51.4$), where

$$EVI_{max_{S(y)}} = 0.771(SPEI9_{Sep}) + 0.712 \quad (8)$$

Table 3. Comparison of the late 20th century (1980–1999) climate conditions with conditions in the early 21st century (2000–2013) at the eight study sites.

Biome	Site	Consecutive dry years 2000–2013	Consecutive dry years 1980–1999	Warm season ΔT (°C)	Cool season ΔT (°C)	Warm season ΔP (mm)	Cool season ΔP (mm)
Forest	US-Fuf	5	1	0.73	0.49	−62.61	−42.13
	US-Vcm	8	1	1.54	0.90	−88.54	−43.48
	US-Vcp	8	1	1.47	0.82	−84.62	−40.48
	Mean Forest Sites			**1.25**	**0.74**	**−78.59**	**−42.03**
Shrubland	US-Srm	8	2	0.81	0.45	−39.19	−85.73
	US-Ses	6	3	0.66	0.05	−27.76	−10.05
	US-Whs	6	2	0.75	0.35	−5.88	−60.03
	Mean Shrubland Sites			**0.74**	**0.29**	**−24.28**	**−51.93**
Grassland	US-Wkg	6	2	0.67	0.23	−12.62	−78.50
	US-Seg	6	3	0.65	0.05	−25.14	−7.50
	Mean Grassland Sites			**0.66**	**0.14**	**−18.88**	**−43.00**

Notes: "Consecutive Dry Years" is defined as the number of consecutive years where 12-month SPEI (calculated from 1 km Daymet data) <0. Warm season (April–September) and cool season (October–March) ΔT is defined as the change in temperature (in °C) between the early 21st century and late 20th century mean seasonal temperatures. Warm season and cool season ΔP is the change in precipitation (in mm) between the early 21st century and late 20th century mean seasonal precipitation. Bold values represent the mean warm and cool season ΔP and ΔT by biome.

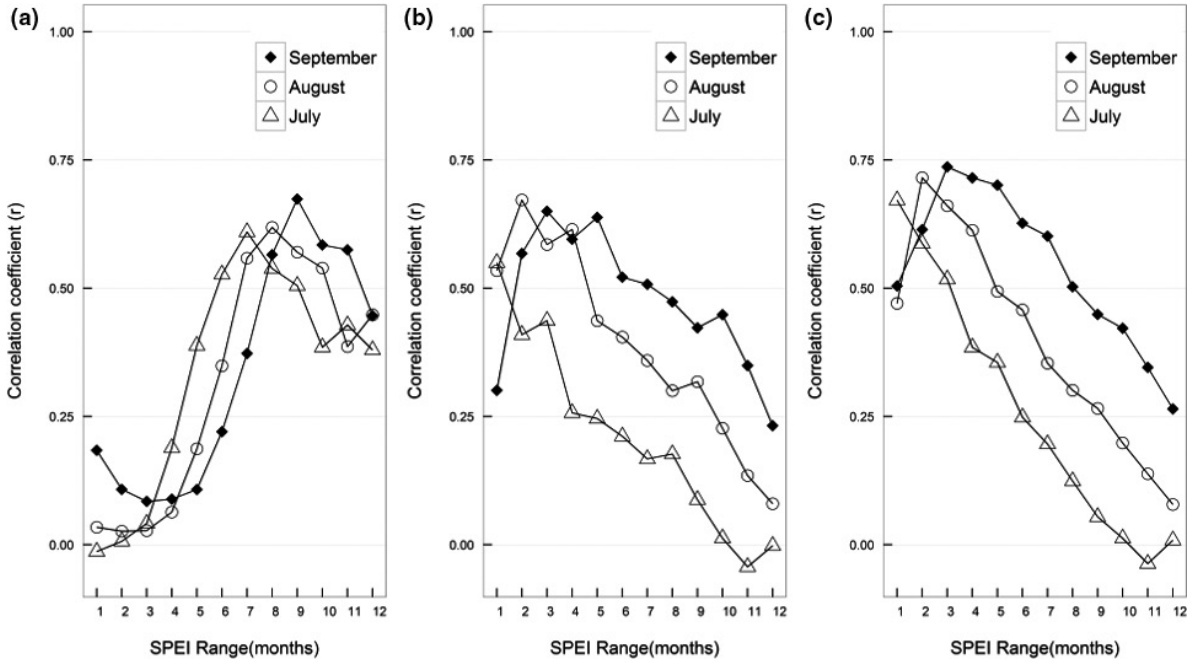

Fig. 4. The dynamic timescale of ecosystem response to combined precipitation and temperature (SPEI) for forests (a), shrublands (b), and grasslands (c). Points represent the correlation coefficient *r* between EVI_{max} and SPEI ranging from 1 to 12 months, calculated back from July, August, and September.

Table 4. Revisit of drought conditions at the dominant timescale for each site.

Biome	Site	Drought years (2000–2013) SPEI annual timescale	Drought years (2000–2013) SPEI dominant timescale	ΔDrought years
Forest ($SPEI9_{Sep}$)	US-Fuf	5	6	1
	US-Vcm	7	9	2
	US-Vcp	7	9	2
Shrubland ($SPEI2_{Aug}$)	US-Srm	6	3	−3
	US-Ses	8	6	−2
	US-Whs	6	6	−2
Grassland ($SPEI3_{Sep}$)	US-Wkg	8	7	−1
	US-Seg	6	5	−1

Notes: The number of years of drought (SPEI < −0.5) as determined by SPEI at the annual timescale (October–September) is compared to the number of drought years for the dominant timescale. The difference between the number of drought years using SPEI at the dominant timescale and annual SPEI is also represented. Positive values of "ΔDrought Years" indicates there were more drought years defined by the dominant timescale of SPEI than annual SPEI, and negative values indicate there were fewer drought years defined by the dominant timescale.

explained 45% of the variance in $EVIs_{max_{(y)}}$ with a root mean squared error (RMSE) = 0.572 for the residuals of modeled vs. measured $EVIs_{max_S}$ (Fig. 5a).

For Southwest shrublands, the most parsimonious model (AIC_c = 93.3) was based on SPEI calculated in August at a 2-month timescale ($SPEI2_{Aug,}$ representing the cumulative water balance from July to August) (Table 5). The selected model,

$$EVI_{max_{S(y)}} = 0.668(SPEI2_{Aug}) \quad (9)$$

explained 45% of the variance in $EVIs_{max_{(y)}}$ and the residuals of modeled vs. measured values of EVI_{max_S} resulted in an RMSE = 0.712 (Fig. 5b).

For Southwest grasslands, the model with best results was based on SPEI calculated in September at a 4-month timescale ($SPEI3_{Sep}$ representing the cumulative water balance from July to September) (AIC_c = 61.3) (Table 5). The other three models were much less parsimonious, and were not selected. The selected model,

$$EVI_{max_{S(y)}} = 0.660(SPEI3_{Sep}) \quad (10)$$

explained 54% of the variance in $EVI_{S_{max}}$ and the residuals of modeled vs. measured values of EVI_{max_S} resulted in an RMSE = 0.650 (Fig. 5c). Notably, the previous-year's EVI_{max} was not a significant predictor of the current year's EVI_{max} in grasslands, shrublands or forests.

In summary, all three selected models were based on SPEI, which accounts for both precipitation and temperature at the dominant timescale for each biome. The ability of the SPEI to explain interannual variation in EVI_{max_S} could indicate: (1) the effect of temperature on the water balance (as reflected by SPEI) explains variation in EVI_{max_S} beyond the simple combination of precipitation and temperature; or (2) SPEI, because it accounts for the effects of sub-annual climate dynamics on production, identifies the critical time period during which climate dynamics influence interannual variation in EVI_{max}. To identify whether variation in EVI_{max_S} was primarily explained by (1) SPEI itself or (2) the dominant timescale as identified by the SPEI, we tested the SPEI model against precipitation and temperature over the timescale of the most parsimonious SPEI model. In forests, the model based on precipitation in January through September ($P9_{Sep}$) was more parsimonious than the model based on either $SPEI9_{Sep}$ or $P9_{Sep}$ combined with $T_{max9_{Sep}}$ (ΔAIC_c = −1.3 and 0.2; Table 6). Similarly, in shrublands the most parsimonious model was based solely on precipitation; precipitation in July and August ($P2_{Aug}$) was a better model than $SPEI2_{Aug}$ or $P2_{Aug}$ combined with $T_{max2_{Aug}}$ (ΔAIC_c = 5.4 and 2.5; Table 6). In grasslands, $P3_{Sep}$ combined with $T_{max3_{Sep}}$ was the more parsimonious than $P3_{Sep}$ alone or $SPEI3_{Sep}$ (ΔAIC_c = 5.4 and 1.3; Table 6). Overall, differences in explanatory power of models based on SPEI, precipitation, and combined precipitation and temperature were small within the dominant timescale for each biome. These results suggest that climate dynamics within the dominant timescale, rather than the SPEI, predominantly explained interannual variation in EVI_{max_S}.

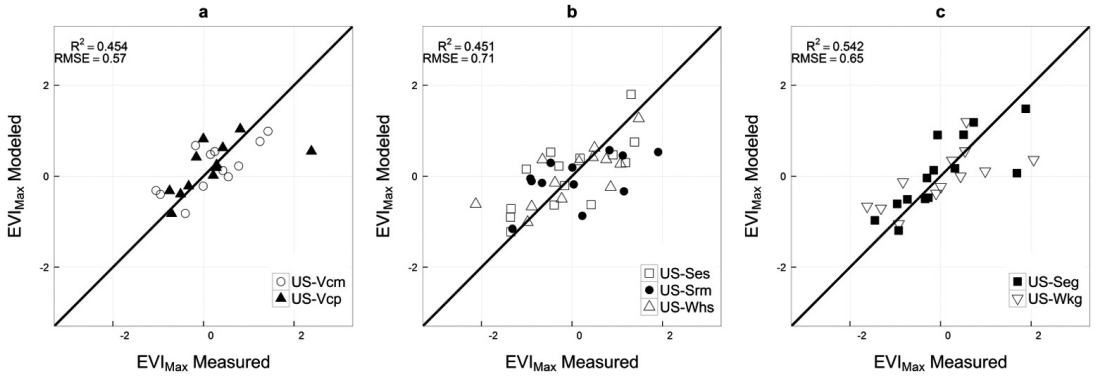

Fig. 5. Relation between measured and modeled standardized maximum Enhanced Vegetation Index (EVI) (EVI_{max_S}) and the most parsimonious model for each biome. (a) Forest model based on Eq. 8 ($SPEI9_{Sep}$) based on two forest sites (US-Vcm, US-Vcp), (b) Shrubland model based on Eq. 9 ($SPEI2_{Aug}$) based on 3 shrubland sites (US-Ses, US-Srm, US-Whs), and (c) Grassland model based on Eq. 10 ($SPEI3_{Sep}$) based on 2 grassland sites (US-Seg, US-Wkg). RMSE is the root mean squared error of the difference between measured and modeled EVI_{max}.

Table 5. Comparison of models predicting current year peak EVI ($EVI_{max_{S(y)}}$) as a function of current year precipitation ($P_{TS(y)}$), previous year peak EVI ($EVI_{max_{S(y-1)}}$), and SPEI at the three timescales with the maximum correlation with EVI_{max_S} (see Figs. 5–7). Selected models are shown in boldface.

Biome	Model	AIC_c	ΔAIC_c	r^2
Forest n = 24	**$SPEI9_{Sep}$**	**51.4**	**0**	**0.45**
	$P_{TS(y)} + EVI_{max_{S(y-1)}}$	57.7	6.3	0.22^{ns}
	$P_{coolS} + T_{max_{warmS}}$	57.9	6.5	0.29
	$P_{TS(y)}$	59	7.6	0.15^{ns}
Shrubland n = 39	**$SPEI2_{Aug}$**	**93.3**	**0**	**0.45**
	$P_{TS(y)} + EVI_{max_{S(y-1)}}$	98.1	4.8	0.25
	$P_{coolS} + T_{max_{warmS}}$	107.3	14	0.22
	$P_{TS(y)}$	111.6	18.3	0.07^{ns}
Grassland n = 26	**$SPEI3_{Sep}$**	**61.3**	**0**	**0.54**
	$P_{cool\ S} + T_{max_{warmS}}$	71.2	9.9	0.32
	$P_{TS(y)} + EVI_{max_{S(y-1)}}$	75.9	14.6	0.08^{ns}
	$P_{TS(y)}$	76.8	15.5	0.07^{ns}

Notes: AIC_c is Akaike's information criterion corrected for small sample sizes. Models are ranked by ΔAIC_c, from zero to higher values. If ΔAIC_c values for two candidate models differed by <2, we selected the model with the fewest parameters. Italicized r^2 values with the superscript "ns" were nonsignificant ($P > 0.05$). AIC_c values for nonsignificant models are italicized.

Table 6. Comparison of models predicting current year EVI_{maxS} as a function of SPEI at the dominant timescale for each biome compared to precipitation, and precipitation and temperature models for the corresponding timescale. Selected models are shown in boldface.

Biome	Model	AIC_c	ΔAIC_c	r^2
Forest	$SPEI9_{Sep}$	51.4	0	0.45
	$P9_{Sep}$	**52.7**	**1.3**	**0.35**
	$P9_{Sep} + T_{max9_{Sep}}$	52.9	1.5	0.42
Shrubland	**$P2_{Aug}$**	**87.9**	**0**	**0.49**
	$P2_{Aug} + T_{max2_{Aug}}$	90.4	2.5	0.49
	$SPEI2_{Aug}$	93.3	5.4	0.45
Grassland	**$P3_{Sep}$+$T_{max3_{Sep}}$**	**60**	**0**	**0.56**
	$SPEI3_{Sep}$	61.3	1.3	0.52
	$P3_{Sep}$	65.4	5.4	0.4

Notes: AIC_c is Akaike's information criterion corrected for small sample sizes. Models are ranked by ΔAIC_c, from zero to higher values. Selected models are shown in boldface. If ΔAIC_c values for two candidate models differed by <2, we selected the model with the fewest parameters.

Discerning mechanisms

Of the models based on Eqs. 4–7, the most parsimonious models for forest, shrublands and grasslands were all based on sub-annual SPEI. However, further examination of the effect of precipitation, temperature, and SPEI on EVI_{max_S} (Table 6) suggested that climate dynamics within the dominant timescale, rather than SPEI, were the key drivers of interannual variation in vegetation production. Therefore, our efforts to discern the mechanisms, defined in our introduction as the underlying causes of ecosystem functional responses, were focused on disentangling the effects of precipitation and temperature during the dominant timescale for each biome as defined by SPEI analysis (see Table 5), recognizing that plant physiology and biogeochemical interactions further underlie these relationships. In forests, the dominant timescale was January through September, in shrublands the dominant timescale was July and August; and in grasslands, the dominant

timescale was July through September. We also explored the effect of atmospheric demand (VPD) on production.

In forests, the relative importance of precipitation and temperature shifted throughout the dominant timescale (January–September) (Fig. 6a). In the latter half of the cool season (January–April), both precipitation and daily T_{max} were strongly correlated with standardized maximum GEP (GEP_{max_S}) (r = 0.89 and r = −0.93, respectively). Soil moisture recharge in Southwest forests generally depends on winter precipitation (Swetnam and Betancourt 1998). Warm temperatures in early spring lead to earlier snowmelt and an earlier onset of the growing season (Barnett et al. 2005). In the warm season (May–September), daily T_{max} was negatively correlated with GEP_{max_S} (r = −0.64), and precipitation had little effect (r = 0.26). Additionally, both cool season and warm season VPD was negatively related to GEP_{max_S} (r = −0.88 and r = −0.97, respectively). On the basis of Williams et al. (2013), we evaluated the relationship between daily maximum temperature and daily production in May, June, and July and found a break point in mean daily T_{max} for the forest site, US-Fuf (Fig. 7). At temperatures below 17°C, daily GEP was positively related to temperature, but at temperatures above 17°C, daily maximum temperature was negatively related to GEP. The two separate linear regressions with this breakpoint explained 43% of the variance in daily GEP in May, June and July. Overall, these results support the importance of cool-season precipitation and warm-season temperature and VPD on Southwest forest productivity.

In shrublands, EVI_{max} was most strongly linked with the 2-month SPEI in July and August. This time period coincided with the strong monsoon rains in these ecosystems. At US-Whs, the correlation between July/August precipitation and GEP_{max_S} was stronger than the correlation between T_{max} and GEP_{max_S} (r = 0.93, and r = −0.70, respectively) (Fig. 6b). Correlations between climate drivers and GEP_{max_S} during the rest of the year were weaker. The correlation of VPD in July and August on GEP_{max_S} was strong (r = −0.87), but VPD throughout the rest of the year had little effect on GEP_{max_S}. At US-Srm, the correlation between July/August T_{max} and GEP_{max_S} was stronger than the correlation between precipitation and GEP_{max_S} (r = 0.67 and r = −0.78, respectively). Temperature and precipitation throughout the rest of the year had little correlation with GEP_{max_S} (Fig. 6c). VPD in July and August had a strong negative correlation on GEP_{max_S} (r = −0.78), but there was little relationship between VPD in other months and GEP_{max_S}.

During the dominant timescale (July–September) at Kendall Grassland (US-Wkg), the correlation between precipitation and GEP_{max_S} was strong in both July/August and September/October (r = 0.68 and r = 0.69, respectively). The influence of T_{max} and VPD on GEP_{max_S} was strongest in July and August (r = −0.50 and r = −0.67, respectively), and weak in September/October (Fig. 6d). Exploration of the effect of VPD on daily GEP by month revealed a nonlinear but negative relationship between VPD and GEP, where GEP was very low or zero at high VPD, however, July was the only month where VPD regularly exceeded 3kPA (Fig. 8). Daily GEP was negatively influenced by VPD, but the strength of the negative effect was strongest in July, early in the growing season. In 2006, US-Wkg experienced a drought-induced vegetation transition from native grasses, to a flush of forbs, to eventual establishment of invasive grasses in 2007 and beyond (Scott et al. 2010). Although the vegetation transition is a potential confounding factor, the site was dominated by grasses in every year in the study period except 2006. To preserve temporal continuity, 2006 was included in the analysis.

The effects of the 21st-century drought on biomes across the U.S. Southwest

In studies of Southwest plant communities during the 21st century drought, research has predominantly focused on the effects of reduced precipitation on growth. Our work shows that there are critical sub-annual climate periods during which precipitation and temperature interact to influence vegetation production across biomes. This indicates that the interaction between precipitation and temperature impacts plant communities across biomes in the Southwest. Our results underscore the need to integrate the effect of temperature on the water balance in models of interannual production, even in ecosystems commonly thought to be largely influenced by precipitation, such as grasslands. In addition, our results underscore

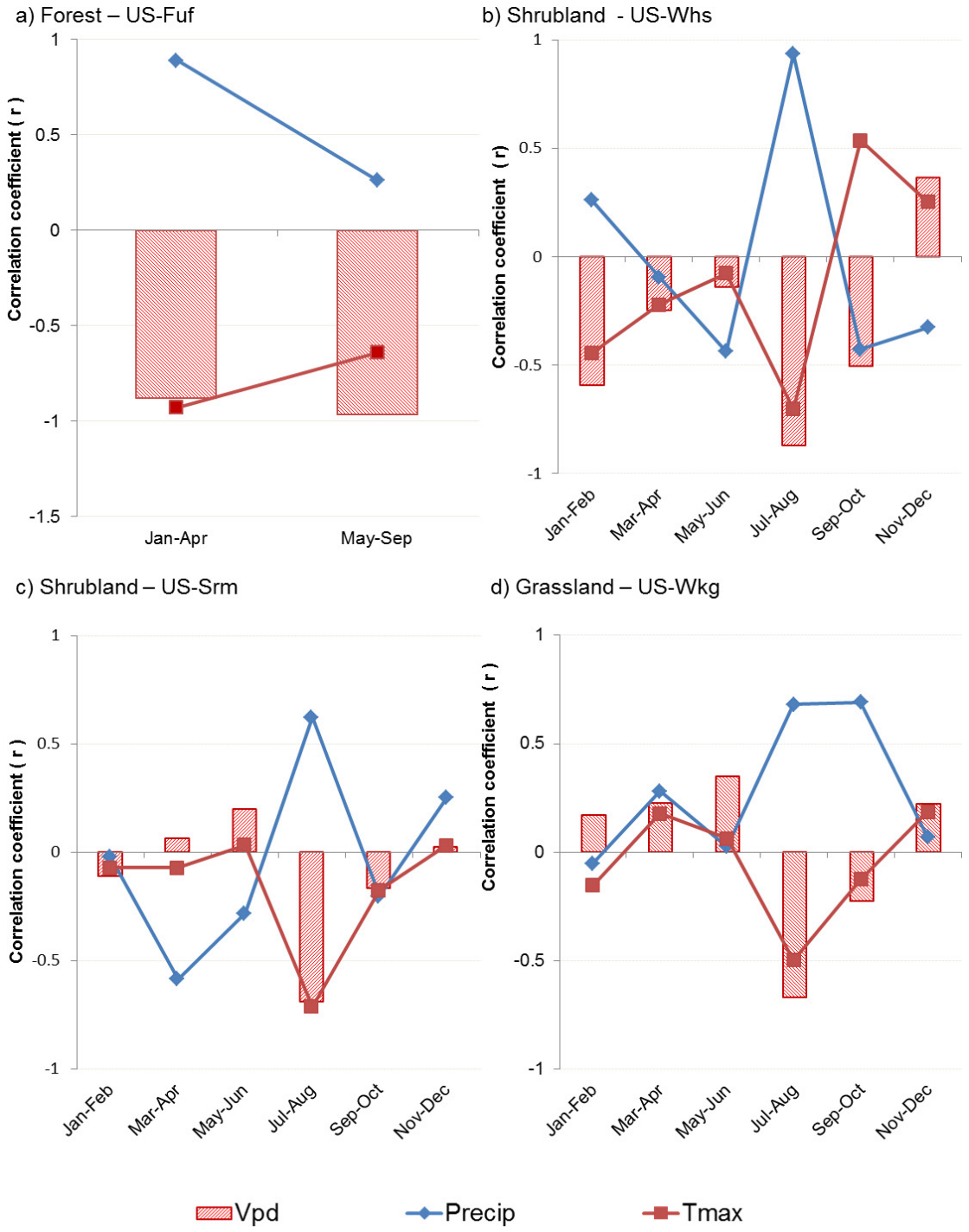

Fig. 6. The correlation coefficient r between daily climate variables (P, T_{max}, and VPD, vapor pressure deficit) and standardized maximum gross ecosystem production (GEP) (GEP_{max_S}) integrated over various time intervals in forests (a), shrublands (b and c), and grasslands (d). Forests had a longer dominant timescale and thus longer integration intervals were used in forest analyses (a). Points represent the correlation coefficient r between climate drivers (precipitation and T_{max}) and GEP_{max_S}. Bars represent the correlation coefficient between VPD and GEP_{max_S}.

the importance of the intra-annual dynamics of climate drivers. Peak production was related to sub-annual SPEI in forests, shrublands, and grasslands, suggesting that intra-annual climate dynamics, rather than annual conditions, influence growth. Furthermore, our results indicate that ecosystem phenology is an important factor in assessing the impact of drought on productivity. A revisit of drought conditions at the dominant timescale indicated that Southwest forests have suffered more severe drought than shrublands or grasslands, which may further explain the decline of Southwest forests during the 21st century drought (Williams et al. 2013). Overall, an improved understanding of interannual variability in production across biomes was provided by the inclusion of the effect of temperature on the water balance and the consideration of the dominant timescale.

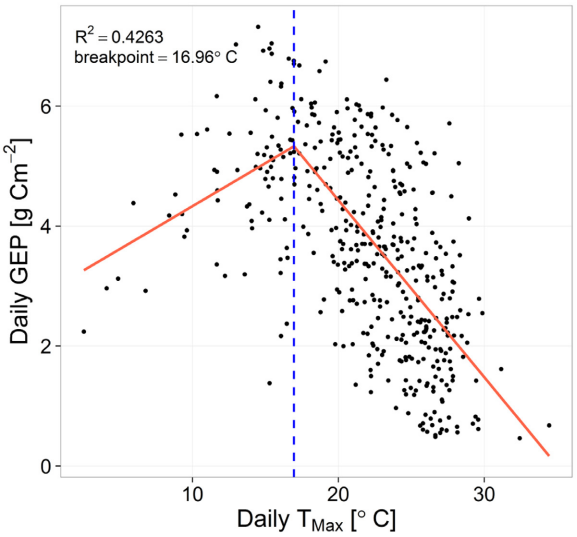

Fig. 7. Scatterplot of daily gross ecosystem production (GEP) against daily maximum temperature (T_{max}) in May, June, and July measured at the US-Fuf site. Lines are fits from linear regression models. Vertical dashed line represents statistically determined breakpoint.

Understanding the empirical relationships underlying these ecosystem functional responses provided further insight into the sub-annual climate dynamics. We focused here on inter- and intra- annual changes in GEP and ecosystem phenology as ecological mechanisms. Site-level GEP correlations with climate drivers indicated that forest production was driven by cool season precipitation but constrained by high warm

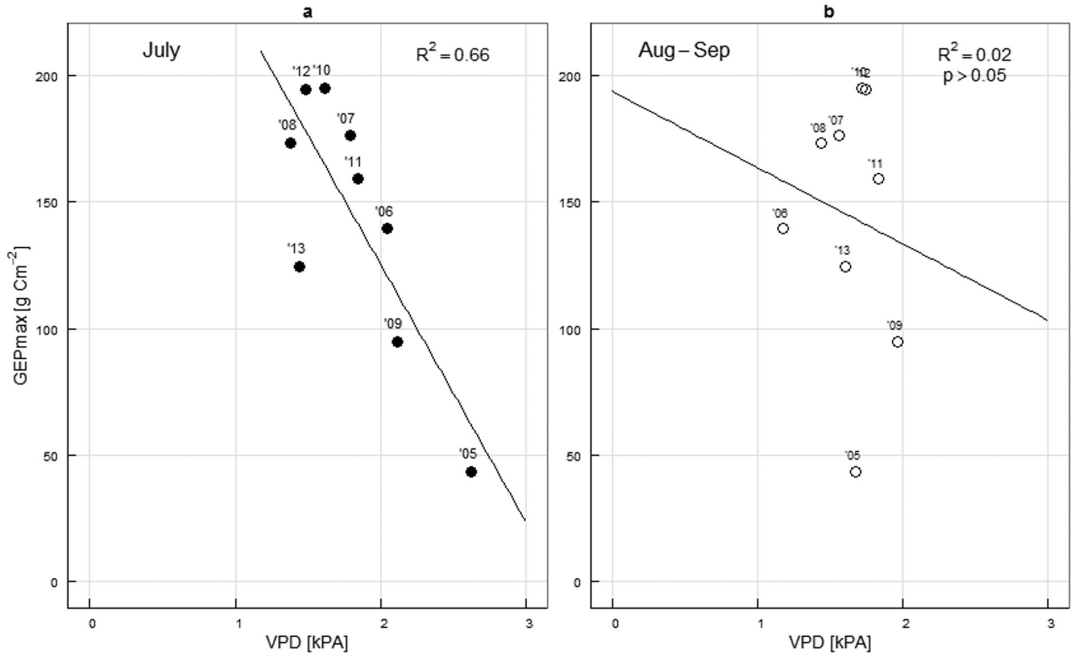

Fig. 8. The relationship between GEP_{max} and VPD during July (a) and August and September (b) at the US-Wkg (Kendall Grassland) site. The coefficient of determination (R^2) for each relationship is in the top right corner of each panel. Years are next to data points.

season temperatures. In shrublands and grasslands, production was driven by summer precipitation and constrained by high warm season temperatures. Grasslands and shrublands operated at similar dominant timescales, though the timescale for grasslands was slightly longer than that of shrublands (3 months vs. 2 months). Compared to other biomes, grasslands respond quickly to even small precipitation events through rapid carbon upregulation and regrowth (Hamerlynck et al. 2010, Scott et al. 2010). This quick response may allow them to be more responsive to late growing season precipitation, thus explaining the longer time scale. Grassland and shrubland production were both constrained by high VPD and temperature. However they differed subtly: in grasslands, the negative effect of high VPD and temperature was strongest early in the growing season in July, while in shrublands, the negative effect of high VPD and temperature was strong throughout the dominant timescale (July–August). Small increases in temperature have an exponential effect on VPD, which is reflected in the strong negative correlation between VPD and GEP_{max_S} throughout the dominant timescale for all biomes.

The use of satellite observations of vegetation greenness to approximate ANPP has been a common practice over the past 30 yr (e.g., Goward et al. 1985 to Zhang et al. 2015). The theoretical basis for this link is based on the direct relationship between the interaction of solar radiation with the plant canopy and vegetation production (Huete et al. 2015). Many studies use vegetation indices as surrogates for ANPP (e.g., Ponce-Campos et al. 2013, Zhang et al. 2013, Moran et al. 2014). In situ measurements of ANPP result in uncertainties due to inconsistent sampling procedures across and within sites (Sala et al. 1988) and variability in the timing of peak greenness (Huete et al. 2015). Satellite measurements can provide greater temporal stability and less spatial uncertainty than plot-scale ANPP measurements in cross-site, long-term studies (Moran et al. 2014). Although we do not claim EVI_{max} is a surrogate for ANPP, the importance of sub-annual climate dynamics likely extends to ANPP.

The mechanisms controlling plant-water relations exert strong controls on the feedback between vegetation and climate via the carbon, water, and energy balance of the ecosystem. The projected future terrestrial carbon sink varies considerably depending on which land surface model makes the projection (Friedlingstein et al. 2014) and an assessment of eight models from the coupled model intercomparison project (CMIP5) indicates that model differences in the carbon uptake response to temperature, precipitation, and soil moisture are an important part of this variation (Shao et al. 2013). The empirical relationships evident from this study (Tables 5 and 6) indicate that the effects of temperature and moisture on carbon gain in arid ecosystems are not easily separated. However they provide an opportunity to evaluate different models, as different hypothesized relationships between the carbon and hydrological cycles. In carrying out these evaluations we recommend that carbon water relationships at sub-annual timescales should be explored. Insofar as EVI can be used as a proximate ecosystem response variable, the availability of soil moisture estimates from NASA's Soil Moisture Active Passive (SMAP) allows our findings to be explored for some ecosystems across large geographic areas more suited to comparison with land surface models.

Overall, this study identified the existence of critical climatic timescales that influence productivity across biomes. Within these dominant timescales, consideration of the effects of temperature in addition to precipitation allowed us to improve predictions of plant functional responses to climate. Predicted higher temperatures in the Southwest will increase evaporative demand (Breshears et al. 2013) and drought severity (Cayan et al. 2010). Our results suggest that the co-occurrence of drought and high temperatures during critical sub-annual periods could reduce annual production, regardless of climate conditions throughout the rest of the year.

Concluding Remarks

This work has uncovered convergences in the timing and relative importance of climate drivers of productivity across the forest-to-grassland continuum in the southwest United States. Interpretation of model results with flux data underscores the importance of investigating climate drivers at multiple temporal scales. Examination of daily GEP yielded important insights into the effects of temperature on

production underlying the annual model results. The coupled approach (remotely sensed observations and in situ flux measurements) has the potential to generalize the functional responses of vegetation to predicted future climate conditions.

Acknowledgments

The research was partly funded by the NASA SMAP Science Definition Team under agreement 08-SMAPSDT08-0042, and the NASA SMAP Science Team under agreement NNH14AX72I. We also acknowledge Dr. Marcy Litvak, who contributed tower data for the US-Vcm, US-Vcp, US-Ses, and US-Seg towers to the AmeriFlux data archive (http://ameriflux.ornl.gov/). Funding for AmeriFlux core site data and data resources was provided by the U.S. Department of Energy's Office of Science. This manuscript was greatly improved by comments from David D. Breshears and Joel A. Biederman and we thank them for their contributions.

Literature Cited

Adams, H. D., M. Guardiola-Claramonte, G. A. Barron-Gafford, J. C. Villegas, D. D. Breshears, C. B. Zou, P. A. Troch, and T. E. Huxman. 2009. Temperature sensitivity of drought-induced tree mortality portends increased regional die-off under global-change-type drought. Proceedings of the National Academy of Sciences USA 106:7063–7066.

Allen, C. D., et al. 2010. A global overview of drought and heat-induced tree mortality reveals emerging climate change risks for forests. Forest Ecology and Management 259:660–684.

Backlund, P., A. Janetos, and D. Schimel. 2008. The effects of climate change on agriculture, land resources, water resources, and biodiversity. Synthesis and assessment product 4.3, U.S. Climate Change Science Program, Washington, D.C., USA.

Barnett, T. P., J. C. Adam, and D. P. Lettenmaier. 2005. Potential impacts of a warming climate on water availability in snow-dominated regions. Nature 438:303–309.

Beguería, S., and S. M. Vicente-Serrano. 2013. SPEI: calculation of the standardised precipitation-evapotranspiration index. R package version 1.6. http://CRAN.R-project.org/package=SPEI

Breshears, D. D., et al. 2005. Regional vegetation die-off in response to global-change-type drought. Proceedings of the National Academy of Sciences USA 102:15144–15148.

Breshears, D. D., H. D. Adams, D. Eamus, N. G. McDowell, D. J. Law, R. E. Will, A. P. Williams, and C. B. Zou. 2013. The critical amplifying role of increasing atmospheric moisture demand on tree mortality and associated regional die-off. Frontiers in Plant Science 4:1–4.

Burnham, K. P., and D. R. Anderson. 2002. Model selection and multimodel inference: a practical information-theoretic approach. Springer-Verlag, New York, New York, USA.

Cayan, D. R., T. Das, D. W. Pierce, T. P. Barnett, M. Tyree, and A. Gershunov. 2010. Future dryness in the southwest US and the hydrology of the early 21st century drought. Proceedings of the National Academy of Sciences USA 107:21271–21276.

Craine, J. M. 2013. The importance of precipitation timing for grassland productivity. Plant Ecology 214:1085–1089.

Craine, J. M., A. Joern, E. G. Towne, and R. G. Hamilton. 2009. Consequences of climate variability for the performance of bison in tallgrass prairie. Global Change Biology 15:772–779.

Craine, J. M., J. B. Nippert, A. J. Elmore, A. M. Skibbe, S. L. Hutchinson, and N. A. Brunsell. 2012. Timing of climate variability and grassland productivity. Proceedings of the National Academy of Sciences USA 109:3401–3405.

Dore, S., T. E. Kolb, M. Montes-Helu, B. W. Sullivan, W. D. Winslow, S. C. Hart, J. P. Kaye, G. W. Koch, and B. A. Hungate. 2008. Long-term impact of a stand-replacing fire on ecosystem CO_2 exchange of ponderosa pine forests. Global Change Biology 14:1–20.

Easterling, D. R., G. A. Meehl, C. Parmesan, S. A. Changnon, T. R. Karl, and L. O. Mearns. 2000. Climate extremes: observations, modeling, and impacts. Science 289:2068–2074.

Fang, J., S. Piao, Z. Tang, C. Peng, and W. Ji. 2001. Interannual variability in net primary production and precipitation. Science 293:1723–1723.

Friedlingstein, P., M. Meinshausen, V. K. Arora, C. D. Jones, A. Anav, S. K. Liddicoat, and R. Knutti. 2014. Uncertainties in CMIP5 climate projections due to carbon cycle feedbacks. Journal of Climate 27:511–526.

Goward, S. N., C. J. Tucker, and D. G. Dye. 1985. North American vegetation patterns observed with the NOAA-7 advanced very high resolution radiometer. Vegetatio 64:3–14.

Hamerlynck, E. P., R. L. Scott, M. S. Moran, T. O. Keefer, and T. E. Huxman. 2010. Growing season ecosystem and leaf-level gas exchange of an exotic and native semiarid bunchgrass. Oecologia 163:561–570.

Hsu, J. S., J. Powell, and P. B. Adler. 2012. Sensitivity of mean annual primary production to precipitation. Global Change Biology 18:2246–2255.

Huete, A., K. Didan, T. Miura, E. P. Rodriguez, Z. Gao, and L. G. Ferreira. 2002. Overview of the radiometric and biophysical performance of the MODIS vegetation indices. Remote Sensing of Environment 83:195–213.

Huete, A., G. Ponce-Campos, Y. Zhang, N. Restrepo-Coupe, X. Ma, and M. S. Moran. 2015. Monitoring photosynthesis from space. Pages 3–22 *in* P. Thenkabail, editor. Remote sensing handbook. Volume 2. Taylor & Francis, Boca Raton, Florida, USA.

Huxman, T. E., K. A. Snyder, D. Tissue, A. J. Leffler, K. Ogle, W. T. Pockman, D. R. Sandquist, D. L. Potts, and S. Schwinning. 2004. Precipitation pulses and carbon fluxes in semiarid and arid ecosystems. Oecologia 141:254–268.

IPCC. 2013. Climate change 2013: the physical science basis. Pages 1–1535 *in* T. Stocker, D. Qin, G. Plattner, M. Tignor, S. Allen, J. Boschung, A. Nauels, Y. Xia, V. Bex, and P. Midgley, editors. Contribution of Working Group I to the Fifth Assessment Report of the Intergovernmental Panel on Climate Change. Cambridge University Press, Cambridge, UK.

Jenerette, G. D., G. A. Barron-Gafford, A. J. Guswa, J. J. McDonnell, and J. C. Villegas. 2012. Organization of complexity in water limited ecohydrology. Ecohydrology 5:184–199.

Jönsson, P., and L. Eklundh. 2004. TIMESAT—a program for analyzing time-series of satellite sensor data. Computers & Geosciences 30:833–845.

Kerhoulas, L. P., T. E. Kolb, and G. W. Koch. 2013. Tree size, stand density, and the source of water used across seasons by ponderosa pine in northern Arizona. Forest Ecology and Management 289:425–433.

Knapp, A. K., and M. D. Smith. 2001. Variation among biomes in temporal dynamics of aboveground primary production. Science 291:481–484.

Lauenroth, W. K., and O. E. Sala. 1992. Long-term forage production of North American shortgrass steppe. Ecological Applications 2:397.

Ma, X., et al. 2013. Spatial patterns and temporal dynamics in savanna vegetation phenology across the North Australian Tropical Transect. Remote Sensing of Environment 139:97–115.

MacDonald, G. M. 2010. Water, climate change, and sustainability in the southwest. Proceedings of the National Academy of Sciences USA 107:21256–21262.

Mazerolle, M. J., 2013. AICcmodavg: Model selection and multimodel inference based on (Q)AIC(c). R package version 1.35. http://CRAN.R-project.org/pacakge=AICcmodavg

Moran, M. S., et al. 2014. Functional response of U.S. grasslands to the early 21st-century drought. Ecology 95:2121–2133.

Moran, M. S., D. P. C. Peters, M. P. McClaran, M. H. Nichols, and M. B. Adams. 2008. Long-term data collection at USDA experimental sites for studies of ecohydrology. Ecohydrology 1:377–393.

Mueggo, V. M. R., 2008. Segmented: an R Package for fit regression models with broken-line relationships. R. News, 8/1, 20-205. http://cran.r-project.org/doc/Rnews/

Peters, D. P. C., J. Yao, O. E. Sala, and J. P. Anderson. 2012. Directional climate change and potential reversal of desertification in arid and semiarid ecosystems. Global Change Biology 18:151–163.

Peters, D. P. C., J. Yao, D. Browning, and A. Rango. 2014. Mechanisms of grass response in grasslands and shrublands during dry or wet periods. Oecologia 174:1323–1334.

Ponce-Campos, G. E., et al. 2013. Ecosystem resilience despite large-scale altered hydroclimate conditions. Nature 494:349–352.

R Core Team. 2013. R: a language and environment for statistical computing. R Foundation for Statistical Computing, Vienna, Austria.

Reichmann, L. G., O. E. Sala, and D. P. C. Peters. 2013. Precipitation legacies in desert-grassland primary production occur through previous-year tiller density. Ecology 94:435–443.

Running, S. W., R. R. Nemani, and R. D. Hungerford. 1987. Extrapolation of synoptic meteorological data in mountainous terrain and its use for simulating forest evapotranspiration and photosynthesis. Canadian Journal of Forest Research 17:472–483.

Sala, O. E., W. J. Parton, L. A. Joyce, and W. K. Lauenroth. 1988. Primary production of the central grassland region of the United States. Ecology 69:40–45.

Sala, O. E., L. A. Gherardi, L. G. Reichmann, E. G. Jobbagy, and D. P. Peters. 2012. Legacies of precipitation fluctuations on primary production: theory and data synthesis. Proceedings of the Royal Society of London. Series B, Biological Sciences 367:3135–3144.

Scott, R. L., E. P. Hamerlynck, G. D. Jenerette, M. S. Moran, and G. A. Barron-Gafford. 2010. Carbon dioxide exchange in a semidesert grassland through drought-induced vegetation change. Journal of Geophysical Research 115:G03026.

Seager, R., et al. 2007. Model projections of an imminent transition to a more arid climate in Southwestern North America. Science 316:1181–1184.

Seager, R., and G. A. Vecchi. 2010. Greenhouse warming and the 21st century hydroclimate of southwestern North America. Proceedings of the National Academy of Sciences USA 107:21277–21282.

Shao, P., X. Zeng, K. Sakaguchi, R. K. Monson, and X. Zeng. 2013. Terrestrial carbon cycle: climate relations in eight CMIP5 Earth system models. Journal of Climate 26:8744–8764.

Sims, D. A., E. R. Brzostek, A. F. Rahman, D. Dragoni, and R. P. Phillips. 2014. An improved approach for remotely sensing water stress impacts on forest C uptake. Global Change Biology 20:2856–2866.

Swetnam, T. W., and J. L. Betancourt. 1998. Mesoscale disturbance and ecological response to decadal climatic variability in the American Southwest. Journal of Climate 11:3128–3147.

Thornthwaite, C. W. 1948. An approach toward a rational classification of climate. Geographical Review 38:55–94.

Thornton, P. E., S. W. Running, and M. A. White. 1997. Generating surfaces of daily meteorological variables over large regions of complex terrain. Journal of Hydrology 190:214–251.

Vicente-Serrano, S. M., S. Beguería, and J. I. López-Moreno. 2010. A multiscalar drought index sensitive to global warming: the standardized precipitation evapotranspiration index. Journal of Climate 23:1696–1718.

Vicente-Serrano, S. M., S. Beguería, J. Lorenzo-Lacruz, J. J. Camarero, J. I. López-Moreno, C. Azorin-Molina, . 2012. Performance of drought indices for ecological, agricultural, and hydrological applications. Earth Interactions 16:1–27.

Vicente-Serrano, S. M., C. Gouveia, J. J. Camarero, S. Beguería, R. Trigo, J. I. López-Moreno, C. Azorín-Molina, E. Pasho, J. Lorenzo-Lacruz, and J. Revuelto. 2013. Response of vegetation to drought time-scales across global land biomes. Proceedings of the National Academy of Sciences USA 110:52–57.

Weiss, J. L., C. L. Castro, and J. T. Overpeck. 2009. Distinguishing pronounced droughts in the southwestern United States: seasonality and effects of warmer temperatures. Journal of Climate 22:5918–5932.

Williams, A. P., et al. 2013. Temperature as a potent driver of regional forest drought stress and tree mortality. Nature Climate Change 3:8–13.

Zhang, Y., et al. 2013. Extreme precipitation patterns and reductions of terrestrial ecosystem production across biomes. Journal of Geophysical Research. Biogeosciences 118:148–157.

Zhang, Y., M. Voigt, and H. Liu. 2015. Contrasting responses of terrestrial ecosystem production to hot temperature extreme regimes between grassland and forest. Biogeosciences 12:549–556.

Zhao, M., and S. W. Running. 2010. Drought-induced reduction in global terrestrial net primary production from 2000 through 2009. Science 329:940–943.